Metal-assisted electrochemical etching of silicon

2010 Nanotechnology 21 465301

(http://iopscience.iop.org/0957-4484/21/46/465301)

Nanotechnology **21** (2010) 465301 (6pp) doi:10.1088/0957-4484/21/46/465301

Metal-assisted electrochemical etching of silicon

Z P Huang[1,3], N Geyer[2,3], L F Liu[2], M Y Li[1] and P Zhong[1]

[1] Functional Molecular Materials Center, Scientific Research Academy, Jiangsu University, Zhenjiang 212013, People's Republic of China
[2] Max Planck Institute of Microstructure Physics, Weinberg 2, D-06120 Halle/Saale, Germany

E-mail: zphuang@ujs.edu.cn and ngeyer@mpi-halle.mpg.de

Received 11 August 2010, in final form 13 September 2010
Published 25 October 2010
Online at stacks.iop.org/Nano/21/465301

Abstract
In this paper the metal-assisted electrochemical etching of silicon is introduced. By electrochemical measurement and sequent simulation, it is revealed that the potential of the valence band maximum at the silicon/metal interface is more negative than that of the silicon/electrolyte interface. Accordingly, holes injected from the back contact are driven preferentially to the silicon/metal interface. Consequently, silicon below metal is electrochemically etched much faster than a naked silicon surface without metal coverage. Metals such as Ag and Cu have been utilized to catalyze the electrochemical etching. Feature sizes as small as 30 nm can be achieved by metal-assisted electrochemical etching. Meanwhile, the metal-assisted electrochemical etching method enables convenient control over the etching direction of non-(100) substrates, and facilitates the fabrication of orientation-modulated silicon nanostructures.

1. Introduction

Silicon (Si) nanostructures have exhibited promising application potential in fields ranging from advanced electronics [1, 2], opto-electronics [3], to energy harvesting [4] and storage [5, 6], to chemical- and biosensors [7, 8], to name a few. Correspondingly, low cost fabrication methods enabling the morphological control of Si nanostructures are of importance because the mass production of the desired Si nanostructures is essential for their wide applications. Among many candidates, top-down wet etching methods (e.g. electrochemical etching [9, 10] and metal-assisted chemical etching [11, 12]) might be promising because of their simplicity and versatility. These methods have been successfully utilized to fabricate Si wires or pores with feature sizes ranging from several microns to sub 10 nm [13–17]. Nowadays, researchers continue to pay attention to improving these methods because there are some factors limiting the application of the two methods.

In the anodic electrochemical etching of Si, a well-known $2 \times W$ rule limits the smallest feature size of etched structures at least in the area of macroporous silicon etching [18, 14], where W is the width of the space charge layer. Consequently, the feature sizes of structures fabricated by the electrochemical etching of Si are usually larger than several hundred nanometers, due to the $2 \times W$ rule [18, 14], or smaller than 5 nm, due to a quantum wire effect [19]. In the metal-assisted chemical etching of Si, only noble metals (Pt, Pd, Au, Ag) can be practically utilized to assist the etching of Si [11, 12, 20]. Moreover, wet etching of Si usually proceeds anisotropically. Namely, the etching prefers to proceed along the ⟨100⟩ directions in anodic electrochemical etching [18, 21] and metal-assisted chemical etching [22–26]. A current source effect [27, 28] has been found in the electrochemical etching of Si, revealing that the etching would occur toward the direction of the current source if the current density is sufficiently high. Such an effect, however, has not been found in pores smaller than 3 μm [28]. Several methods has been developed to suppress the anisotropy in metal-assisted chemical etching [17, 29, 30], e.g. by increasing the lateral size of the metal mask [17] or changing the concentration of oxidant in the etchant [30]. Nevertheless, the control is trivial and time consuming [30].

Therefore, a method enabling wide range size control, convenient orientation control of Si nanostructures, and possibly cost control is yet to be developed. In this paper, a method combining electrochemical etching and metal-assisted chemical etching is introduced. Although this method has been tentatively utilized to affect the etching direction of

[3] Authors to whom any correspondence should be addressed.

non-(100) Si substrates [30], the mechanism, merit, and features of the metal-assisted electrochemical etching method have not yet been explored. By electrochemical measurement and simulation, it is revealed that the current is driven to the Si/metal interface when a Si substrate loaded with metal particles is subjected to electrochemical etching in an aqueous HF solution. On the basis of this finding, the metal-assisted electrochemical etching of Si is developed. Features with a size as small as 30 nm can be obtained by this method. Both Ag and Cu can be used to assist the etching of Si. Moreover, the method enables easy control over the etching directions of non-(100) substrates.

2. Experimental details

The Si wafers used in the experiments were p type (100) and (111) wafers (ρ: 1–10 Ω cm, Silicon Materials, Landsberg am Lech, Germany). The wafers were cut into 2 × 2 cm^2 pieces, degreased by ultrasonic cleaning in acetone for 10 min, subjected to boiling RCA solution for 30 min, and dipped into diluted aqueous HF solution for 1 min. Afterward, the Si substrates, of which the back side was scratched by indium–gallium (InGa) alloy (99.99%, Sigma-Aldrich) to achieve Ohmic contact, were assembled into a home-made electrochemical cell. The InGa-alloy-scratched back side of Si substrates was in contact with a copper plate. In the electrochemical cell only the front surface of Si substrates was exposed to the solution during the metal plating and the sequent electrochemical etching. The plating solution was composed of HF (4.6 M), deionized water, and $AgNO_3$ (20 mM) or $Cu(NO_3)_2$ (20 mM). The metal plating was performed under front side room light illumination at room temperature. The metal-loaded substrates were electrochemically etched in a two-electrode setup with a platinum wire as a counter electrode. The etching was performed in an aqueous HF (3.4 wt%) solution in the dark at room temperature under galvanostatic conditions, with a Keithley 2430 source meter as a current source. An electrochemical workstation (CH Instrument, 614D) was utilized to measure the open circuit potential and capacitance–voltage relation. The morphologies of the substrates were characterized by scanning electron microscope (SEM, JEOL 6701).

3. Results and discussion

The surface barrier height (SBH) and potential of valence band maximum (PVBM) were analyzed by combining electrochemical measurement and numeric simulation to explore the possibility of using metal particles as a catalyzer in the electrochemical etching of Si. The SBH of a Si substrate (Φ) in etchant, a mixture solution containing HF and H_2O, can be deduced from measurable parameters (i.e. open circuit potential (OCP or V_{OC}), the flat band potential of a bare Si substrate (V_{fb}), and the energy difference between the Fermi level and the PVBM in the bulk of a p-type Si substrate (V_n)) according to the relation $\Phi = V_{bb} + V_n = V_{fb} - V_{OC} + V_n$ [31], where V_{bb}, defined as $V_{bb} = V_{fb} - V_{OC}$, is the band bending behind Si without metal coverage under open circuit conditions.

The OCPs of a bare Si substrate without any metal coverage, as well as of Si substrates subjected to an Ag-plating solution for 30 s and 120 s, respectively, were experimentally measured. As shown by figure 1(a), when a Si substrate is loaded with Ag particles (30 s plating), the apparent OCP of the substrate shifts positively, compared to a bare Si substrate. The shift becomes pronounced as the metal coverage is increased by raising the plating time from 30 to 120 s (figure 1(a)). The positive shift of the apparent OCP exhibits the influence of Ag coverage on the apparent SBH of the Si substrate in the etchant. The apparent OCP is contributed by the SBH on both the Si/electrolyte interface and the Si/Ag interface in a partially Ag-covered Si substrate. Accordingly, the actual difference between the SBH of Si with ($\Phi_{Si/Ag}$) and without ($\Phi_{Si/electrolyte}$) Ag coverage, Δ, should be extracted from the difference between the OCP of a Si fully covered by Ag particles ($V_{OC,Si/Ag}$) and the OCP of a fresh Si substrate without any metal coverage ($V_{OC,Si/electrolyte}$). That is, $\Delta = \Phi_{Si/Ag} - \Phi_{Si/electrolyte} = V_{OC,Si/electrolyte} - V_{OC,Si/Ag}$. In our experiment, a Si substrate subjected to 120 s plating was fully covered by the deposited Ag particles. Accordingly, the OCPs presented in figure 1(a) give that Δ is −0.184 V.

The PVBM relative to a reference electrode, a Pt wire in our experiments, can be approximately described by equation (1) in cylindrical coordinates (ρ, θ, z) modified from the models developed by Tung [32] and Rossi [33]:

$$V(\rho, z) = V_a + V_n + V_{bb}\left(1 - \frac{z}{W}\right)^2 + \sum_{i=1}^{n} \frac{\Delta}{2\pi} \times \int_0^{2\pi}\int_0^{R_i} \frac{\rho_1 z}{[z^2+(\rho-\rho_i)^2+\rho_1^2-2(\rho-\rho_i)\rho_1\cos(\theta_1)]^{3/2}}\,\mathrm{d}\rho_1\,\mathrm{d}\theta_1 \quad (1)$$

where ρ is defined on the surface of substrate; the z axis is along the surface normal into the substrate; V_a is the bias applied on a Si substrate relative to the reference electrode; V_n is given by $V_n = \frac{kT}{e}\ln(\frac{N_V}{N_A})$; k is the Boltzmann constant; T is the Kelvin temperature; e is the elementary charge; N_A and N_V are the acceptor density and effective density of states in the valence band, respectively; W is given by $(2\varepsilon_0\varepsilon V_{bb}/eN_A)^{1/2}$; ε_0 is the permittivity of free space; ε is the dielectric constant of the Si material; n is the amount of circular Ag patches; ρ_i is the center coordinate of Ag patch i on the surface of the substrate; and R_i is the diameter of Ag patch i. N_A and V_{fb} can be obtained by the fitting of the Mott–Schottky plot with the relationship $\frac{1}{C_{sc}^2} = \frac{2}{e\varepsilon\varepsilon_0 N_A}(V_a - V_{fb} - \frac{kT}{e})$ [34]. The capacitances of the space charge layer in a bare Si substrate, C_{sc}, were measured at different applied biases and presented in a Mott–Schottky plot in figure 2(b). The fitting of the Mott–Schottky plot gives that V_{fb} is −0.388 V and N_A is 1.616 × 10^{15} cm^{-3}. With V_{fb} and N_A known, the PVBM in the space charge region of a Si substrate in contact with Ag patches can be computed according to equation (1).

Figure 1(c) shows the computed PVBM of a Si substrate contacted with a series of 50 nm diameter circular Ag patches under 0.3 V bias, which is approximately the bias used in

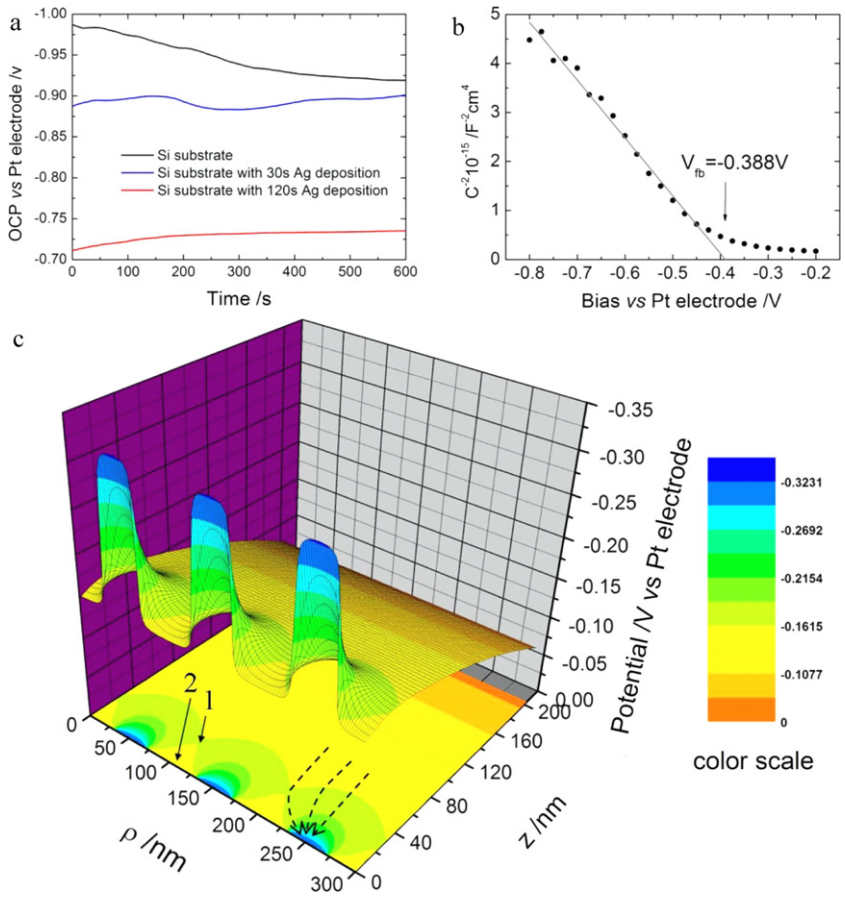

Figure 1. (a) The relation between the OCP and the metal coverage of Si. (b) The Mott–Schottky plot of a bare Si(100) substrate in HF solution. (c) The computed PVBM of a Si substrate in contact with an array of 50 nm diameter Ag patches distributed from $\rho = -450$ to 450 nm with a 100 nm interval. The contour of PVBM is projected on the ρ–z plane.

the metal-assisted electrochemical etching of Si (figure 2). It is clearly revealed by figure 1(c) that the PVBM behind the Ag patches is more negative than the PVBM behind the Si without a Ag contact. Moreover, due to the potential perturbations induced by the Ag patches, the PVBM behind the Si without a contact exhibits potential saddles (as marked by arrow 1 in the contour plot of the PVBM in figure 1(c)) whose potential is more negative than that at the Si/electrolyte surface (as marked by arrow 2 in the contour plot of PVBM in figure 1(c)). Consequently, the holes will be concentrated to the Si/Ag interface when they are injected from the back contact and come near to the surface region of a Si substrate, as illustrated by the broken arrows in the contour plot of the PVBM in figure 1(c). As a result, the oxidation and etching of the Si will occur preferentially at the Si/Ag interface, compared to Si without a metal contact. That is, the etching of the Si below the Si/Ag interface will proceed much faster than the etching that occurs at Si without a metal contact. Meanwhile, the simulation result presented in figure 1(c) shows that the concentration effect occurs even if the clearance between the Ag patches is as small as 50 nm.

The concept of metal-assisted electrochemical etching was confirmed by experiments. A naked Si substrate and a 30 s Ag-plated Si substrate are subjected to galvanostatic electrochemical etching with identical current densities, respectively. The necessary bias applied to the naked Si substrate (the gray line in figure 2(a)) is larger than the bias applied to the 30 s Ag-plated substrate (the black line in figure 2(a)). The smaller bias applied to the 30 s Ag-plated substrate confirms that Ag locating on the surface of the Si substrate can lower the barrier height at the Si/Ag interface, compared to Si/electrolyte interface. Besides the applied bias, the morphologies of the Si substrate loaded with/without metal coverage subjected to the electrochemical etching appear to be different (panels (b)–(d) of figure 2). The Ag-particle-loaded Si substrate developed into nanopores or nanowires extending into the substrate (panels (b) and (c) of figure 2), whereas neither nanowires nor nanopores formed in the etched bare Si substrate. The control experiments confirm unambiguously the catalytic effect of metal particles in the electrochemical etching of Si. Meanwhile, if an Ag-particle-loaded Si substrate was subjected to the same HF aqueous solution as that used in figures 2(b)–(d) for more than 1 h and neither voltage nor current was applied, then no etching of the Si substrate was found. Therefore, the Si pores or wires presented in figures 2(b) and (c) result from the metal-assisted electrochemical etching of Si, but not the electroless etching of Si.

It is clearly shown by the SEM images (panels (b) and (c) of figure 2) that the Ag particles locate at the etching

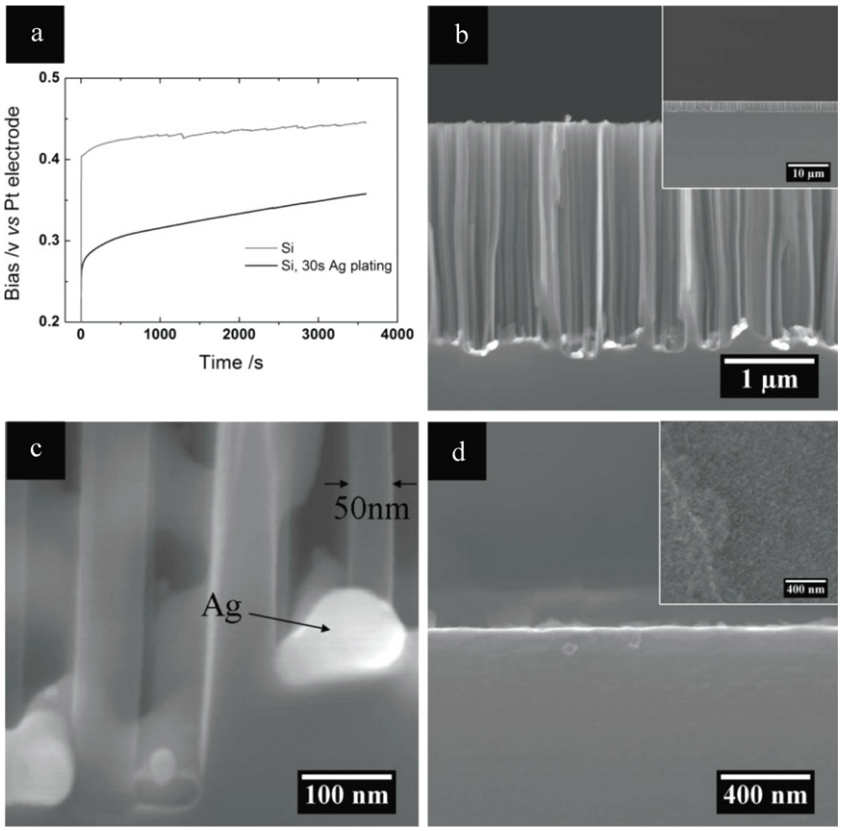

Figure 2. (a) The applied bias on the Si substrates with/without Ag coverage in electrochemical etching experiments. ((b), (c)) Cross-sectional view SEM images of an Ag-particle-loaded Si substrate subjected to electrochemical etching. (d) Cross-sectional view and (inset) plan view SEM images of a bare Si substrate subjected to electrochemical etching.

front (i.e. the bottom of pores), confirming that the etching occurs preferentially at the Si/Ag interface. Metal-assisted electrochemical etching occurs homogeneously on the entire Si substrate with metal coverage, as implied by the inset of figure 2(b). It is worth noting that structures with well-defined sizes as small as 50 nm are obtained (figure 2(c)), although the Si is electrochemically etched in our method. Therefore, the sizes of the Si structures are defined by the clearance between the metal particles, as is the case in the metal-assisted chemical etching of Si, instead of the width of space charge layer.

The analysis concerning different SBHs at the Si/metal interface and the Si/electrolyte interface implies that the electrochemical etching of Si can be catalyzed by a metal with an electrochemical potential more positive than the electrochemical potential of the electrolyte, (i.e. the electrochemical potential of H^+/H_2). To verify this assumption, electrochemical etching of Si was performed with the assistance of Cu particles. The Cu particles were plated onto the Si substrate by subjecting the Si substrate to a mixture solution containing HF and Cu^{2+}. Figure 3(a) and its inset show typical plan view SEM images of a Cu-particle-loaded Si substrate. Cu-assisted electrochemical etching of Si results in nanowires or nanopores on the Si substrate (panels (b) and (c) of figure 3), which look similar to the structures resulting from Ag-assisted electrochemical etching (panels (b) and (c) of figure 2). The Cu particles also locate at the etching front, and nanowires with a diameter as small as 30 nm are obtained. The results shown in figures 2 and 3 confirm the mechanism we proposed. In the metal-assisted chemical etching of Si, holes are supplied by the reduction of the oxidant on the surface of the metal, and usually Cu particles can be oxidized by oxidants (e.g. H_2O_2, Fe^{3+}) and vanish immediately after a short-time incubation in the etchant. Consequently, Cu-assisted chemical etching of Si usually results in shallow pits on the surface of the Si (figure 3(d)) due to the loss of Cu, instead of nanowires or nanopores. Therefore, our finding presented in figure 3 is practically important because it shows for the first time that a relatively cheap metal, Cu, can be utilized to catalyze the etching of Si into nanostructures, which will greatly lower the cost of Si nanostructures from the metal-assisted etching method.

Due to the different back bond strengths of Si atoms on different crystal planes, in wet etchings of a Si substrate the etching proceeds intrinsically anisotropically. A convenient method enabling control over the etching direction of the Si substrate has yet to be developed. In our previous work, we demonstrated that the etching direction in the metal-assisted electrochemical etching of a (111) Si substrate can be affected by the current density [30]. At a low current density, the (111) Si substrate is etched anisotropically in the inclined directions, while the etching proceeds along the surface normal if the current density is sufficiently large. Such phenomena suggest that the orientation-modulated Si nanowire can be conveniently fabricated by metal-assisted electrochemical etching of the Si

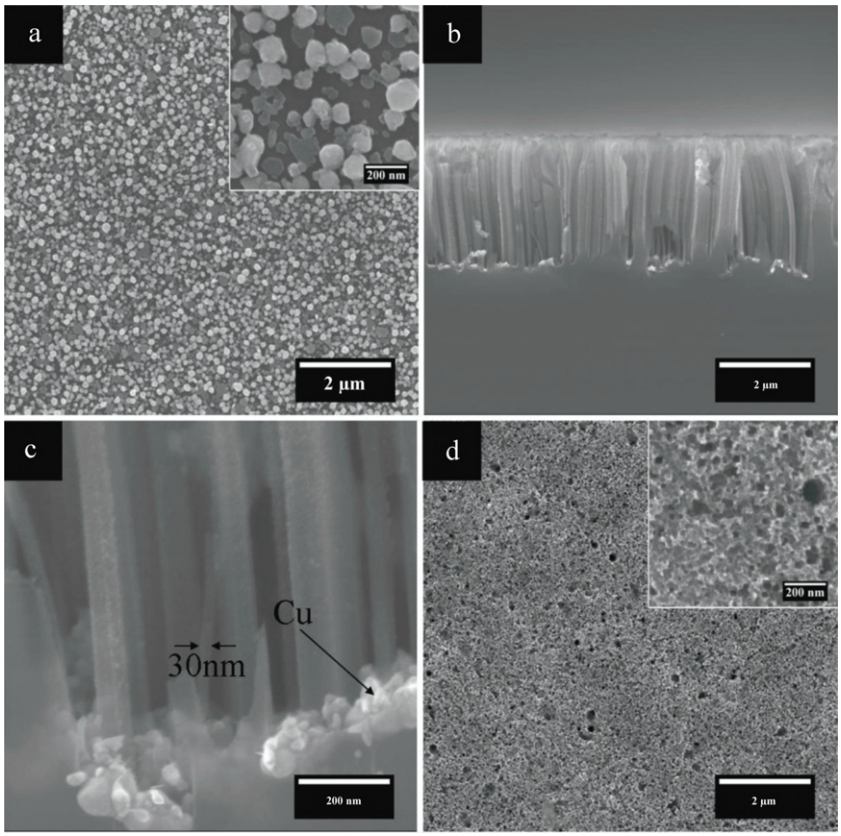

Figure 3. (a) Plan view SEM images of Cu particles loading on a Si substrate. ((b), (c)) Cross-sectional view SEM images of a Cu-loaded Si substrate subjected to electrochemical etching in a HF solution. (d) A plan view SEM image of a Cu-loaded Si substrate subjected to chemical etching in a HF/H_2O_2 solution.

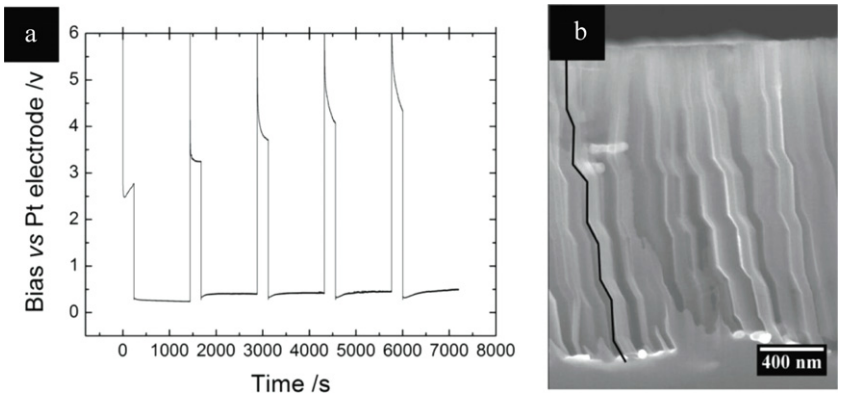

Figure 4. (a) The bias applied on a Ag-loaded Si substrate in the electrochemical etching. Five periods of high (5 mA cm^{-2}) and low (0.2 mA cm^{-2}) density current etching were applied to the Ag-loaded Si substrate. (b) A cross-sectional view SEM image of the orientation-modulated Si nanostructures.

substrate under current–density-modulated conditions. This assumption was confirmed by the etching of an Ag-loaded (111) substrate under periodically low and high current densities. As shown by figure 4, when five periods of high/low density current (figure 4(a)) were applied, the Ag-loaded Si substrate was etched into orientation-modulated wires or pores (figure 4(b)). With the aid of a black line, five periods of vertical etching and inclined etching are clearly shown in figure 4(b).

4. Conclusion

To conclude, the metal-assisted electrochemical etching of Si is investigated by theoretical analysis and electrochemical experiments. Both Ag and Cu exhibit catalytic activity. The size of the features fabricated by metal-assisted electrochemical etching is determined by the clearance between the metal particles, instead of the width of the space charge layer. By periodically varying the density of the

etching current, orientation-modulated Si nanostructures can be conveniently fabricated.

Acknowledgment

The financial support of the research foundation of Jiangsu University, PR China (09JDG043) is greatly acknowledged.

References

[1] Goldberger J, Hochbaum A I, Fan R and Yang P 2006 Silicon vertically integrated nanowire field effect transistors *Nano Lett.* **6** 973–7
[2] Schmidt V, Riel H, Senz S, Karg S, Riess W and Gösele U 2006 Realization of a silicon nanowire vertical surround-gate field-effect transistor *Small* **2** 85–8
[3] Tian B, Zheng X, Kempa T J, Fang Y, Yu N, Yu G, Huang J and Lieber C M 2007 Coaxial silicon nanowires as solar cells and nanoelectronic power sources *Nature* **449** 885–90
[4] Peng K Q, Xu Y, Wu Y, Yan Y J, Lee S T and Zhu J 2005 Aligned single-crystalline Si nanowire arrays for photovoltaic applications *Small* **1** 1062–7
[5] Chan C K, Peng H, Liu G, McIlwrath K, Zhang X F, Huggins R A and Cui Y 2008 High-performance lithium battery anodes using silicon nanowires *Nat. Nanotechnol.* **3** 31–5
[6] Peng K, Jie J, Zhang W and Lee S T 2008 Silicon nanowires for rechargeable lithium-ion battery anodes *Appl. Phys. Lett.* **93** 033105
[7] Cui Y, Wei Q, Park H and Lieber C M 2001 Nanowire nanosensors for highly sensitive and selective detection of biological and chemical species *Science* **293** 1289–92
[8] Patolsky F, Zheng G and Lieber C M 2006 Fabrication of silicon nanowire devices for ultrasensitive, label-free, real-time detection of biological and chemical species *Nat. Protoc.* **1** 1711–24
[9] Lehmann V and Föll H 1990 formation mechanism and properties of electrochemically etched trenches in n-type silicon *J. Electrochem. Soc.* **137** 653–9
[10] Matthias S, Müller F, Jamois C, Wehrspohn R B and Gösele U 2004 Large-area three-dimensional structuring by electrochemical etching and lithography. *Adv. Mater.* **16** 2166–70
[11] Peng K Q, Yan Y J, Gao S P and Zhu J 2002 Synthesis of large-area silicon nanowire arrays via self-assembling nanoelectrochemistry *Adv. Mater.* **14** 1164–7
[12] Peng K Q, Wu Y, Fang H, Zhong X Y, Xu Y and Zhu J 2005 Uniform, axial-orientation alignment of one-dimensional single-crystal silicon nanostructure arrays *Angew. Chem. Int. Edn* **44** 2737–42
[13] Birner A, Wehrspohn R B, Gösele U and Busch K 2001 Silicon-based photonic crystals *Adv. Mater.* **13** 377–88
[14] Kleimann P, Badel X and Linnros J 2005 Toward the formation of three-dimensional nanostructures by electrochemical etching of silicon *Appl. Phys. Lett.* **86** 183108
[15] Huang Z P, Fang H and Zhu J 2007 Fabrication of silicon nanowire arrays with controlled diameter, length, and density *Adv. Mater.* **19** 744–8
[16] Huang Z P, Zhang X X, Reiche M, Liu L F, Lee W, Shimizu T, Senz S and Gösele U 2008 Extended arrays of vertically aligned sub-10 nm diameter [100] Si nanowires by metal-assisted chemical etching *Nano Lett.* **8** 3046–51
[17] Huang Z P, Shimizu T, Senz S, Zhang Z, Zhang X X, Lee W, Geyer N and Gösele U 2009 Ordered arrays of vertically aligned [110] silicon nanowires by suppressing the crystallographically preferred ⟨100⟩ etching directions *Nano Lett.* **9** 2519–25
[18] Lehmann V 1993 The physics of macropore formation in low doped n-type silicon *J. Electrochem. Soc.* **140** 2836–43
[19] Lehmann V and Gösele U 1991 Porous silicon formation: a quantum wire effect *Appl. Phys. Lett.* **58** 656–8
[20] Peng K Q, Hu J J, Yan Y J, Wu Y, Fang H, Xu Y, Lee S T and Zhu J 2006 Fabrication of single-crystalline silicon nanowires by scratching a silicon surface with catalytic metal particles *Adv. Funct. Mater.* **16** 387–94
[21] Christophersen M, Carstensen J and Föll H 2000 *Phys. Status Solidi* a **182** 45
[22] Peng K Q, Zhang M L, Lu A J, Wong N B, Zhang R Q and Lee S T 2007 Ordered silicon nanowire arrays via nanosphere lithography and metal-induced etching *Appl. Phys. Lett.* **90** 163123
[23] Chen C Y, Wu C S, Chou C J and Yen T J 2008 Morphological control of single-crystalline silicon nanowire arrays near room temperature *Adv. Mater.* **20** 3811–5
[24] Fang H, Li X D, Song S, Xu Y and Zhu J 2008 Fabrication of slantingly-aligned silicon nanowire arrays for solar cell applications *Nanotechnology* **19** 255703
[25] Peng K, Lu A, Zhang R and Lee S T 2008 Motility of metal nanoparticles in silicon and induced anisotropic silicon etching *Adv. Funct. Mater.* **18** 3026–35
[26] Zhang M L, Peng K Q, Fan X, Jie J S, Zhang R Q, Lee S T and Wong N B 2008 Preparation of large-area uniform silicon nanowires arrays through metal-assisted chemical etching *J. Phys. Chem.* C **112** 4444–50
[27] Ponomarev E A and Levy-Clement C 1998 Macropore formation on p-type Si in fluoride containing organic electrolytes *Electrochem. Solid State Lett.* **1** 42–5
[28] Lehmann V and Ronnebeck S 1999 The physics of macropore formation in low-doped p-type silicon *J. Electrochem. Soc.* **146** 2968–75
[29] Chen H A, Wang H, Zhang X H, Lee C S and Lee S T 2010 Wafer-scale synthesis of single-crystal zigzag silicon nanowire arrays with controlled turning angles *Nano Lett.* **10** 864–8
[30] Huang Z P, Shimizu T, Senz S, Zhang Z, Geyer N and Gösele U 2010 Oxidation rate effect on the direction of metal-assisted chemical and electrochemical etching of silicon *J. Phys. Chem.* C **111** 10683–90
[31] Morrison S R 1980 *Electrochemistry at Semiconductor and Oxidized Metal Electrodes* (New York: Plenum)
[32] Tung R T 1992 Electron transport at metal–semiconductor interfaces: general theory *Phys. Rev.* B **45** 13509–23
[33] Rossi R C and Lewis N S 2001 Investigation of the size-scaling behavior of spatially nonuniform barrier height contacts to semiconductor surfaces using ordered nanometer-scale nickel arrays on silicon electrodes *J. Phys. Chem.* B **105** 12303–18
[34] Barsoukov E and Macdonald J R 2005 *Impedance Spectroscopy Theory, Experiment, and Applications* (New York: Wiley)